



# Magnitude and Kinetics of T Cell and Antibody Responses During H1N1pdm09 Infection in Inbred Babraham Pigs and Outbred Pigs

Matthew Edmans<sup>1†</sup>, Adam McNee<sup>1†</sup>, Emily Porter<sup>2†</sup>, Eleni Vatzia<sup>1</sup>, Basu Paudyal<sup>1</sup>, Veronica Martini<sup>1</sup>, Simon Gubbins<sup>1</sup>, Ore Francis<sup>2</sup>, Ross Harley<sup>2</sup>, Amy Thomas<sup>2</sup>, Rachel Burt<sup>2</sup>, Sophie Morgan<sup>1</sup>, Anna Fuller<sup>3</sup>, Andrew Sewell<sup>3</sup>, Bryan Charleston<sup>1†</sup>, Mick Bailey<sup>2†</sup> and Elma Tchilian<sup>1\*†</sup>

## OPEN ACCESS

### Edited by:

Vitaly V. Ganusov,  
The University of Tennessee,  
United States

### Reviewed by:

John Driver,  
University of Florida, United States  
Claudia Cicala,  
National Institutes of Health (NIH),  
United States

### \*Correspondence:

Elma Tchilian  
elma.tchilian@pirbright.ac.uk

<sup>†</sup>These authors have contributed  
equally to this work

### Specialty section:

This article was submitted to  
Viral Immunology,  
a section of the journal  
Frontiers in Immunology

**Received:** 10 September 2020

**Accepted:** 15 December 2020

**Published:** 02 February 2021

### Citation:

Edmans M, McNee A, Porter E, Vatzia E, Paudyal B, Martini V, Gubbins S, Francis O, Harley R, Thomas A, Burt R, Morgan S, Fuller A, Sewell A, Charleston B, Bailey M and Tchilian E (2021) Magnitude and Kinetics of T Cell and Antibody Responses During H1N1pdm09 Infection in Inbred Babraham Pigs and Outbred Pigs. *Front. Immunol.* 11:604913. doi: 10.3389/fimmu.2020.604913

<sup>1</sup> The Pirbright Institute, Enhanced Host Responses, Pirbright, United Kingdom, <sup>2</sup> Bristol Veterinary School, University of Bristol, Langford, United Kingdom, <sup>3</sup> Division of Infection and Immunity, Cardiff University School of Medicine, Cardiff, United Kingdom

We have used the pig, a large natural host animal for influenza with many physiological similarities to humans, to characterize  $\alpha\beta$ ,  $\gamma\delta$  T cell and antibody (Ab) immune responses to the 2009 pandemic H1N1 virus infection. We evaluated the kinetic of virus infection and associated response in inbred Babraham pigs with identical MHC (Swine Leucocyte Antigen) and compared them to commercial outbred animals. High level of nasal virus shedding continued up to days 4 to 5 post infection followed by a steep decline and clearance of virus by day 9. Adaptive T cell and Ab responses were detectable from days 5 to 6 post infection reaching a peak at 9 to 14 days.  $\gamma\delta$  T cells produced cytokines *ex vivo* at day 2 post infection, while virus reactive IFN $\gamma$  producing  $\gamma\delta$  T cells were detected from day 7 post infection. Analysis of NP tetramer specific and virus specific CD8 and CD4 T cells in blood, lung, lung draining lymph nodes, and broncho-alveolar lavage (BAL) showed clear differences in cytokine production between these tissues. BAL contained the most highly activated CD8, CD4, and  $\gamma\delta$  T cells producing large amounts of cytokines, which likely contribute to elimination of virus. The weak response in blood did not reflect the powerful local lung immune responses. The immune response in the Babraham pig following H1N1pdm09 influenza infection was comparable to that of outbred animals. The ability to utilize these two swine models together will provide unparalleled power to analyze immune responses to influenza.

**Keywords:** influenza, swine, pig, lung, T cell, Ab, gamma delta cells, H1N1pdm09

## INTRODUCTION

Influenza viruses are a global health threat to humans and pigs, causing considerable morbidity and mortality. Frequent zoonotic crossover between pigs and humans contributes to the evolution of influenza viruses and can be a source for novel pandemic strains (1–3). Human and swine Influenza viruses are prone to interspecies transmission, leading to regular incursions from human to pig and

vice versa generally resulting in an influenza-like illness similar to that of human seasonal influenza (4). The emergence of the 2009 pandemic H1N1 (H1N1pdm09) virus, which is now globally endemic in both pigs and humans, illustrates the importance of pigs in new outbreaks in humans (5). Influenza A virus (IAV) infection in pigs causes significant economic loss due to reduced weight gain, suboptimal reproductive performance and secondary infections. Immunization with inactivated influenza virus is currently the most effective way of inducing strain-specific neutralizing antibodies, directed against the surface glycoprotein hemagglutinin (HA). Because of the constant evolution of the virus, broadly cross-protective vaccines would be highly desirable and central to the control of influenza in both pigs and humans.

Animal models are essential to develop better vaccines and control strategies and to provide insight into human disease. Most models have limitations in recapitulating the full range of disease observed in humans. Mice, guinea pigs and non-human primates are not generally susceptible to natural routes of influenza infection and may require adapted strains, physiologic stressors and/or unnatural inoculation procedures (6–9). In contrast, pigs are an important, natural, large animal host for IAV and are infected by the same subtypes of H1N1 and H3N2 viruses as humans (10, 11). Pigs have a longer life span, are genetically, immunologically, physiologically and anatomically more like humans than small laboratory animals and have a comparable distribution of sialic acid receptors in the respiratory tract (12, 13). Pigs exhibit similar clinical manifestations and pathogenesis when infected with IAV making them an excellent model to study immunity to influenza. Furthermore, we have defined the dynamics of H1N1pdm09 influenza virus transmission in pigs and demonstrated the utility of the pig model to test therapeutic antibody delivery platforms and vaccines (14, 15).

Several inbred miniature pig breeds have been developed, including NIH and Yucatan, with defined swine leukocyte antigens (SLA type, the swine major histocompatibility complex) (16, 17). However, the inbred Babraham is the only example of a full-size inbred strain of pig, closely related to commercial breeds, making them an appropriate model to study diseases important to commercial pig production (18, 19). The sharing of IAV strains between pigs and humans makes it an obvious species in which to study immunity to influenza and to test vaccines or therapeutic strategies prior to human clinical trials. In addition we have developed a toolset to study immune responses in Babrahams, including adoptive cell transfer and peptide SLA tetramers allowing us to study the fine specificity of immune responses (20, 21).

Despite extensive knowledge of the role of T cells in protection against IAV in mice and humans, few studies in pigs have evaluated this in depth. The duration and magnitude of T cell and humoral responses has been assessed after swine H1N1, H1N2, and H3N2 challenges in pigs (22–26). The frequency and activation status of leucocytes in local and systemic tissues was also determined after H1N1pdm09 infection (27). However no detailed analysis of T cell immune responses in broncho-alveolar lavage

(BAL) have been performed, a location which we have shown to contain tissue resident memory cells that are essential for heterosubtypic protection (28). Neither has there been a detailed analysis of T cell and antibody (Ab) immune responses to H1N1pdm09, although this continues to cross the species barrier from humans to pigs. H1N1pdm09 circulating in swine herds maintains antigenic similarity to human seasonal strains, providing a unique opportunity to use a virus affecting both humans and swine to examine immune responses induced by infection.

Here we characterized  $\alpha\beta$ ,  $\gamma\delta$  T cell and Ab immune responses to H1N1pdm09 in local lung and systemic tissues in Babraham pigs and compared them to commercial outbred animals. These two pig models together will allow fine grain dissection of immune responses to IAV in a species which is a natural host for the virus and similar in many respects to humans.

## MATERIALS AND METHODS

### Animals and Influenza H1N1pdm09 Challenge

The animal experiments were approved by the ethical review processes at the Pirbright Institute and Bristol University and conducted according to the UK Government Animal (Scientific Procedures) Act 1986 under project license P47CE0FF2. Both Institutes conform to the ARRIVE guidelines.

Thirty two outbred old Landrace x Hampshire cross (from a commercial high health status herd) and 56 inbred Babraham pigs (bred at Animal Plant Health Agency, APHA Weybridge, UK) were screened for absence of influenza A infection by matrix gene real time RT-PCR and for antibody-free status by HAI using four swine influenza virus antigens - H1N1pdm09, H1N2, H3N2, and avian-like H1N1. The average age of the outbred pigs 7 days before the challenge was 8.7 weeks and of the Babrahams 8.3 weeks. Pigs were challenged intra-nasally with  $1 \times 10^7$  PFU of MDCK grown swine A(H1N1)pdm09 isolate, A/swine/England/1353/2009, derived from the 2009 pandemic virus, swine clade 1A.3. (H1N1pdm09) in a total of 4 ml (2 ml per nostril) using a mucosal atomization device MAD300 (MAD, Wolfe-Tory Medical). Two experiments with outbred (OB) pigs (referred to as OB1 and OB2) and two with inbred Babraham (BM) pigs (referred to as BM1 and BM2) were performed (**Figure 1A**). In each experiment one pig was culled on days 1 to 7, 9, 11, and 13 post infection and a *post-mortem* examination performed with collection of tissue samples. Uninfected controls were sampled: two on the day prior to infection and two at day 8 post infection. Two naïve pigs (referred to as in-contact) were co-housed with the directly challenged pigs in experiments OB1, OB2, BM1, BM2 and culled at days 11 and 13 post infection together with the last two directly challenged pigs. A fifth experiment was performed with Babraham pigs (experiment BM3) in which three were culled on days 6, 7, 13, 14, 20, and 21 post infection (**Figure 1A**). In the BM3 experiment six control animals were included, three of which were culled 1 day before and three on the day of infection.

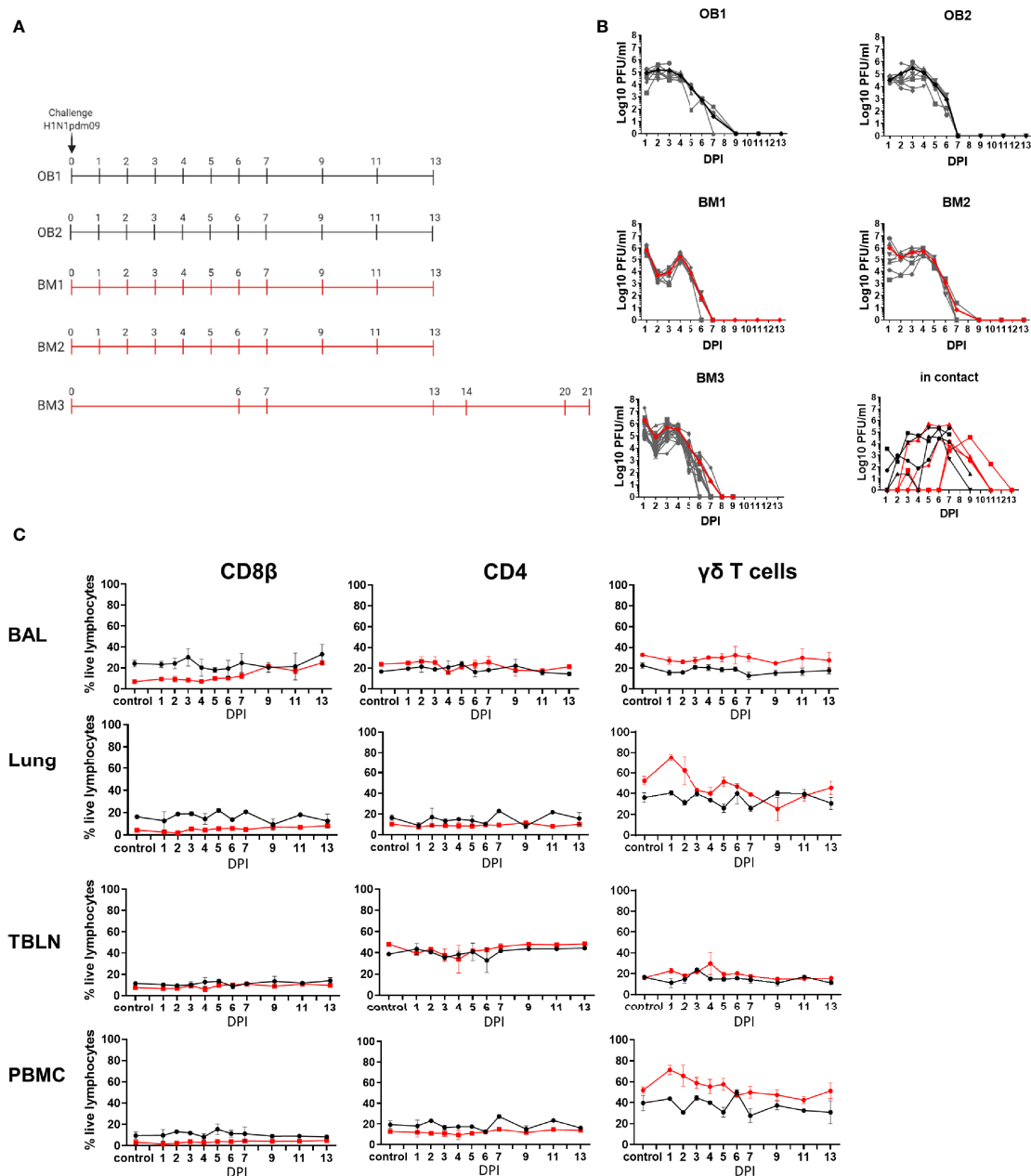


**FIGURE 1** | Experimental design, viral load and cell subset dynamics following H1N1 pdm09 infection. **(A)** Pigs were infected with H1N1pdm09 and culled on the days indicated. Two experiments with outbred (OB1 and OB2, black line) and two with inbred Babraham pigs (BM1 and BM2, red line) were performed. Two in-contact animals were included in each experiment one culled at day 11 and one at day 13 post infection. An extended time course of 21 days was performed with 18 inbred Babraham pigs (BM3, red line) with animals culled on the indicated days. **(B)** Virus load was determined by plaque assay of daily nasal swabs at the indicated time points. The thick line indicates the mean. **(C)** Proportions of CD4, CD8, and  $\gamma\delta$  T cells were determined by flow cytometry at the indicated time points.

## Tissue Sample and Processing

Two nasal swabs (one per nostril) were taken from all surviving pigs following infection with H1N1pdm09 (**Figure 1**) on days 1 to 7, 9, 11, and 13 in OB1, OB2, BM1, and BM2, and on days 1 to 9 in BM3. Animals were humanely euthanized at the indicated times with an overdose of pentobarbital sodium anesthetic.

Peripheral blood (PBMC), tracheobronchial lymph nodes (TBLN), lung, bronchial alveolar lavage (BAL) were processed as previously described (28, 29). The tissue homogenate was washed, red blood cells lysed and cell suspension passed through 100  $\mu$ m cell strainer twice. Cells were cryopreserved in FBS containing 10% DMSO.

## Plaque Assays

Virus titer in nasal swabs was determined by plaque assay on MDCK cells (Central Service Unit, The Pirbright Institute, UK). Samples were 10-fold serially diluted in Dulbecco's Modified Eagle's Medium (DMEM) and 200  $\mu$ l overlaid on confluent MDCK cells in 12 well tissue culture plates. After 1 h, the plates were washed and overlaid with 2 ml of culture medium containing 0.66% Agar. Plates were incubated at 37°C for 48 to 72 h and plaques visualized using 0.1% crystal violet. Plaques were counted at the appropriate dilution and expressed as plaque forming units (PFU) per ml of nasal swab.

## IFN $\gamma$ ELISpot Assay

Frequencies of IFN $\gamma$  spot forming cells (SFC) were determined using cryopreserved cells as previously described (28, 29). Cells were stimulated with live MDCK-grown H1N1pdm09 (MOI 1), medium control, or 4  $\mu$ g/ml Con A (Sigma-Aldrich). Results were expressed as number of IFN $\gamma$  producing cells per 10<sup>6</sup> cells after subtraction of the average number of spots in medium control wells.

## Flow Cytometry

Cryopreserved single cell suspensions from blood, TBLN, BAL and lung were thawed, rested for 1 to 2 h and aliquoted into 96 well plates at 1  $\times$  10<sup>6</sup> cells/well. Cells were stimulated with live MDCK-grown H1N1pdm09 (MOI 1) or medium control and incubated at 37°C for 18 h. Golgi plug (BD Biosciences) was added for the last 4 h of stimulation. PMA Ionomycin (Biolegend) was added to appropriate control wells as a positive control at the same time as the Golgi plug. Following incubation cells were washed at 1,000g for 5 min and re-suspended followed by addition of primary antibodies, Near-Infrared Fixable LIVE/DEAD stain (Invitrogen) and secondary antibodies (Table 1). Unstimulated controls were stained with the same antibodies and their response deducted. For *ex vivo* staining, gating was set by the response in the naïve animals which was negligible (Cells were fixed and permeabilized with BD Fix and perm buffer (BD Biosciences) as per the manufacturer's instructions prior to the addition of internal cytokine antibodies. Cells were washed and re-suspended in PBS prior to analysis using a MACSquant analyser10 (Miltenyi).

The NP<sub>290-298</sub> SLA tetramer binding was performed as previously described (20). Briefly, biotinylated NP peptide loaded SLA monomers, were freshly assembled into tetramer with streptavidin BV421 (Biolegend, UK) and diluted with PBS to a final concentration of 0.1  $\mu$ g/ $\mu$ l. Two million mononuclear cells were incubated with protease kinase inhibitor (Dasatinib, Axon Medchem) in PBS for 30 min at 37°C and 0.3  $\mu$ g of tetramer was added to the cells on ice for another 30 min. Surface staining with optimal antibody concentrations in FACS buffer (PBS supplemented with 2% FCS and 0.05% sodium azide) was performed on ice for 20 min (Table 1). Responses with SLA matched non-influenza tetramers were used as controls and deducted (Supplementary Figure 7). Samples were washed twice with FACS buffer and fixed in 1% paraformaldehyde before analysis on MACSquant analyser10 (Miltenyi). All flow cytometry data was analyzed by Boolean gating using FlowJo v10.6 (TreeStar, US).

## Serological Assays

ELISA was performed using live H1N1pdm09 virus or recombinant hemagglutinin from H1N1pdm09 (pH1) containing a C-terminal thrombin cleavage site, a trimerization sequence, a hexahistidine tag and a BirA recognition sequence as previously described (30). Cut-off values determined as average naïve values plus three-fold standard deviation at optimal starting dilution. Starting dilutions were 1:20, 1:2, and 1:4 for serum, BAL and nasal swab respectively. Hemagglutination inhibition (HAI) Ab titers were determined using 0.5% chicken red blood cells and H1N1pdm09 at a concentration of 4 HA units/ml. Microneutralization (MN) was performed using standard procedures as described previously (15, 31).

The porcine sera were also tested for binding to MDCK-SIAT1 cells stably expressing pH1 from H1N1pdm09 (A/England/195/2009), H1 from A/Puerto Rico/8/1934 (PR8, H1N1) and H5 HA (A/Vietnam/1203/2004). Confluent cell monolayers in 96-well microtiter plates were washed with PBS and 50  $\mu$ l of the serum dilution was added for 1 h at room temperature. The plates were washed three times with PBS and 100  $\mu$ l of horseradish peroxidase (HRP)-conjugated goat anti-pig Fc fragment secondary antibody (Bethyl Laboratories, diluted in PBS, 0.1% BSA) was added for 1 h at room temperature. The plates were washed three times with PBS and developed with 100  $\mu$ l/well TMB high sensitivity substrate solution (Biolegend). After 5 to 10 min the reaction was stopped with 100  $\mu$ l 1 M sulfuric acid and the plates were read at 450 and 570 nm with the Cytation3 Imaging Reader (Biotek). The cut off value was defined as the average of all blank wells plus three times the standard deviation of the blank wells.

## Enzyme-Linked Lectin Assay (ELLA)

Neuraminidase inhibiting Ab titers were determined in serum and BAL fluid using an Enzyme-linked lectin assay (ELLA). Ninety six-well microtiter plates (Maxi Sorp, Nunc, Sigma-Aldrich, UK) were coated with 50  $\mu$ l/well of 25  $\mu$ g/ml fetuin and incubated at 4°C overnight. Heat inactivated sera samples were serially diluted in a separate 96-well plate. An equal volume of (H7(Net219) N1(Eng195) S-FLU (H7N1 S-FLU) (kindly provided by Professor Alain Townsend, University of Oxford) was added to each well and incubated at room temperature on a rocking platform for 20 min. The H7N1 S-FLU was titered beforehand in the absence of serum to determine optimal concentration for the assay. Fetuin plates were washed with PBS four times before 100  $\mu$ l/well of the serum/virus mix was transferred and incubated overnight at 37°C. The serum/virus mix was removed, and the plate washed four times with PBS before adding 50  $\mu$ l/well of Peanut Agglutinin-HRP at 1  $\mu$ g/ml and incubating for 90 min at room temperature on a rocking platform. Plates were washed and 50  $\mu$ l/well of TMB High Sensitivity substrate solution (BioLegend, UK) was added. Plates were developed for 6 min, the reaction stopped with 50  $\mu$ l of 1 M H<sub>2</sub>SO<sub>4</sub> and the plates were read at 450 and 630 nm using a Biotek Elx808 reader. Samples were measured as end titer representing the highest dilution with signal greater than cut-off. The cut off value was defined as the average of all blank wells plus three times the standard deviation of the blank wells.

## B Cell ELISpot

B cell ELISpots were performed for the detection and enumeration of antibody-secreting cells in single cell suspensions prepared from different tissues and peripheral blood. ELISpot plates (Multi Screen-HA, Millipore, UK) were coated with 100  $\mu$ l per well of appropriate antigen or antibody diluted in carbonate/bicarbonate buffer for 2 h at 37°C. To detect HA-specific spot-forming cells, plates were coated with 2.5  $\mu$ g per well of recombinant pHA from H1N1pdm09 (A/England/195/2009) and for the enumeration of total IgG-secreting cells with 1  $\mu$ g per well of anti-porcine IgG (mAb, MT421, Mabtech AB, Sweden) or with culture medium supplemented with 10% FBS (media background control). The coated plates were washed with PBS and blocked with 200  $\mu$ l/well 4% milk (Marvel) in PBS. Frozen cell suspensions from different tissues were filtered through sterile 70  $\mu$ M cell strainers, plated at different cell densities in culture medium (RPMI, 10% FBS, HEPES, Sodium pyruvate, Glutamax and Penicillin/Streptomycin) on the ELISPOT plates and incubated for a minimum of 18 h at 37°C in a 5% CO<sub>2</sub> incubator. After incubation the cell suspension was removed, the plates washed once with ice-cold sterile H<sub>2</sub>O and thereafter with PBS/0.05% Tween 20, before incubation with 100  $\mu$ l per well of 0.5  $\mu$ g/ml biotinylated anti porcine IgG (mAb, MT424, Mabtech AB, Sweden) diluted in PBS/0.5% FBS for 2 h at room temperature. Plates were washed with PBS/0.05% Tween 20 and incubated with streptavidin – alkaline phosphatase conjugate (Strep-ALP, Mabtech AB, Sweden). After a final wash, the plates were incubated with AP Conjugate Substrate (Bio-Rad, UK) for a maximum of 30 min. The reaction was stopped by rinsing the plates in tap water and dried before spots were counted.

## Statistical Analysis

All statistical analyses were performed using Prism 8.1.2. The kinetics of viral shedding were analyzed using a linear mixed model. The model included viral titer (log<sub>10</sub> PFU/ml) as the response variable, day post infection (as a categorical variable) and pig type (OB or BM) and an interaction between them as fixed effects and pig ID nested in experiment as random effects. The model was implemented using the lme4 package (32) in R (version 3.6.1) (<https://www.R-project.org/>).

ELISpot data were analyzed using a linear model. The model included log<sub>10</sub> SFC/10<sup>6</sup> cells+1 as the response variable and day post infection (as a categorical variable), source (BAL, lung, PBMC, TBLN) and pig type (OB or BM) and two- and three-way interactions between them as fixed effects. Model simplification proceeded by stepwise deletion of non-significant (P>0.05) terms as judged by *F*-tests. The model was implemented in R (version 3.6.1).

Because of possible non-normality and non-constant variance the percentage of different T cells (NP<sub>290-298</sub> CD8, IFN $\gamma$  CD8 $\beta$ , IL-2 CD8 $\beta$ , TNF CD8 $\beta$ , IFN $\gamma$  CD4, IL-2 CD4, TNF CD4, IFN $\gamma$  CD2  $\gamma\delta$  ex vivo, TNF CD2  $\gamma\delta$  ex vivo, IFN $\gamma$ /TNF CD2  $\gamma\delta$  ex vivo, IFN $\gamma$  CD2  $\gamma\delta$ , TNF CD2  $\gamma\delta$ , IL-17A CD2  $\gamma\delta$ ) from each source (BAL, lung, PBMC, TBLN) and pig type (OB and BM) at each day post infection were analyzed using Kruskal-Wallis tests. If significant (P<0.05), pairwise Wilcoxon rank-sum (also known as Mann-Whitney) tests were used to compare groups. These analyses were implemented in

R (version 3.6.1). A similar approach was used to compare the percentage of different T cells in all sources from inoculated and uninfected control pigs at each time point and in BAL from in-contact and experimentally inoculated pigs (in this case observations from 6 to 11 dpi were combined).

The dynamics of antibody responses were analyzed by fitting logistic growth curves to the data,  $y = \kappa / (1 + \exp(-\beta(t - \delta)))$ , where  $y$  is the log<sub>10</sub> antibody titer,  $t$  is days post infection,  $\kappa$  is the upper asymptote,  $\beta$  is the rate of increase and  $\delta$  is the time of maximum increase. The parameters (i.e.  $\kappa$ ,  $\beta$  and  $\delta$ ) were allowed to vary between BM and OB pigs. Model fitting using the nlme package (<https://CRAN.R-project.org/package=nlme>) in R (version 3.6.1).

## RESULTS

### Experimental Design, Virus Shedding, and Lymphocyte Dynamics During H1N1pdm09 Infection

Five experiments were performed to characterize local and systemic immune responses. In the first four experiments ten pigs were infected intranasally with H1N1pdm09 virus and monitored for clinical signs. One infected pig was culled on each of days 1 to 7, 9, 11, and 13 post infection. A full post-mortem examination was performed and BAL, lung, TBLN and PBMC samples collected. Four uninfected controls were sampled in parallel, two on the day prior to infection and two at day 8 post infection. Two experiments with outbred (OB) pigs (referred to as experiments OB1 and OB2) and two with inbred Babraham (BM) pigs (referred to as BM1 and BM2) were performed (**Figure 1A**). In addition, two naïve pigs (referred to as in-contact pigs) were co-housed with the directly challenged pigs in experiments OB1, OB2, BM1, BM2 and culled at days 11 and 13 post contact. A fifth experiment was carried out with 18 BM (experiment BM3) in which 3 pigs were culled on each of days 6, 7, 13, 14, 20, and 21 post infection (**Figure 1A**). In the BM3 experiment six uninfected controls were sampled, three 1 day before and three on the day of infection.

Viral load was determined in daily nasal swabs taken from both the directly challenged and in-contact pigs (**Figure 1B**). In directly challenged pigs, peak virus load was reached 1 to 3 days post infection (DPI), declined sharply after 4 DPI and was not detectable after 7 DPI. No differences in virus shedding between OB and BM were detected (p=0.65). Although the onset of viral shedding was delayed, most in-contact pigs showed similar kinetics to directly challenged ones, indicating that the natural contact infection is very similar to intra-nasal challenge with mucosal atomization device (MAD).

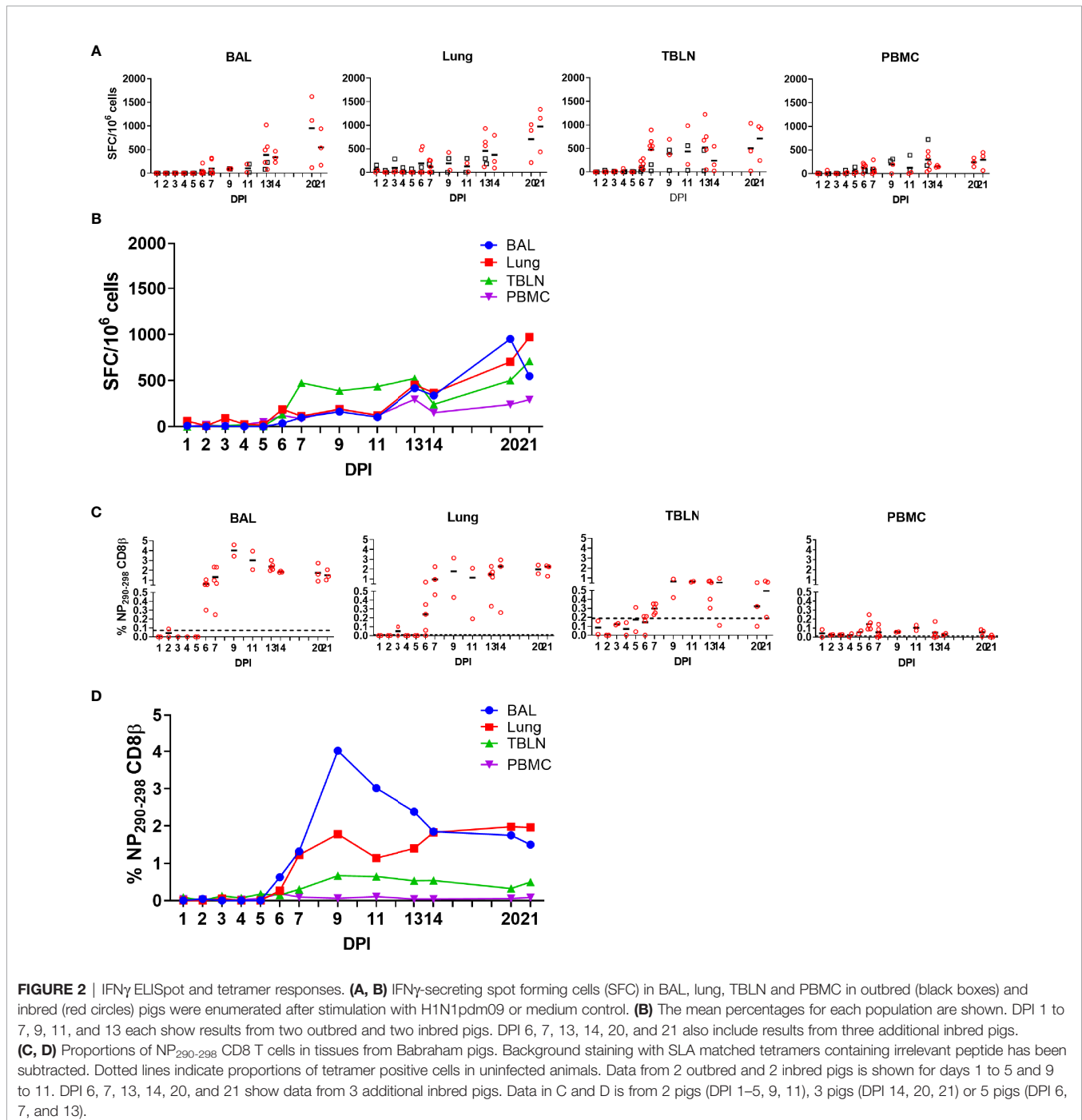
We determined the proportion of CD8 $\beta$ , CD4, and  $\gamma\delta$  T cells over the time course in BAL, lung, TBLN and PBMC (**Figure 1C**, **Supplementary Figure 1**). BM animals had a significantly lower proportion of CD8 $\beta$  T cells than OB, apparent in all tissues in naïve unexposed animals (6.6% in BM vs 24.2% in OB in BAL, 4.2% vs 16.2% in lung, 3.2% vs 9.4% in PBMC and 7.6% vs 11.5% in TBLN) (**Supplementary Figure 1A**). BM animals also showed a significantly higher proportion of  $\gamma\delta$  T cells in BAL, lung and

PBMC (**Supplementary Figure 1A**). No significant differences in CD4 T cells were detected between OB and BM. The proportion of CD4, CD8, and  $\gamma\delta$  T cells did not change significantly over the time course of H1N1pdm09 infection, although an increase in the proportion of CD8 $\beta$  in the BAL for the BM animals was observed, as previously reported (26).

Overall the kinetic of virus infection and shedding were similar between BM and OB, although there were differences in the proportions of CD8 and  $\gamma\delta$  T cells.

## T-Cell Responses During H1N1pdm09 Infection in Pigs

As T cells are crucial for control of virus replication, we examined in detail the CD8 and CD4 responses during H1N1pdm09 infection (33–36). First, we enumerated IFN $\gamma$ -secreting cell by ELISpot following re-stimulation with H1N1pdm09 (**Figures 2A, B**). IFN $\gamma$  spot forming cells (SFC) were detectable from 6 DPI and maintained in all tissues until 21 DPI. During the early stage of infection the strongest responses



were in the TBLN (mean 474 SFC/10<sup>6</sup> cells at 7 DPI), whereas from 14 to 21 DPI the highest number of IFN $\gamma$ -secreting cells was detected in the lung, with SFC continuing to expand in this tissue (mean 368 SFC/10<sup>6</sup> cells at 14 DPI and 972/10<sup>6</sup> cells SFC at 21 DPI). The response in the BAL was lower than lung ( $p=0.04$ ), due to the low proportion of T cells present in the BAL (**Figure 1C**). The IFN $\gamma$  ELISpot response in the PBMC was low with a peak of 296 SFC/10<sup>6</sup> cells at 13 DPI. No differences in responses between the same tissues in OB and BM were detected ( $p > 0.11$ ).

To further dissect the T cell response, we enumerated antigen specific cytotoxic CD8 $\beta$  T cells against the nuclear protein (NP) using peptide NP<sub>290-298</sub> (DFEREGYSL) tetramer, which we have previously shown to be dominant in BM animals infected with H1N1pdm09 (20). Tetramer responses were measured in experiments BM1, BM2, and BM3 (**Supplementary Figure 1B; Figures 2C, D**). NP<sub>290-298</sub> responses were detected in BAL and lung at 6 DPI, reaching a peak at 9 DPI and still present at 20 to 21 DPI. In TBLN one animal responded at 5 DPI, but the peak was at 9 to 11 DPI and still present at 21 DPI. The responses in PBMC were low (0.2% at 6 DPI) and there were no detectable responses at 20 to 21 DPI (**Table 2**).

## Cytokine Production by CD4 and CD8 T Cells

We analyzed production of IFN $\gamma$ , TNF and IL-2 by CD8 $\beta$  and CD4 T cells by intracellular staining (ICS) (**Supplementary Figure 2A**). The kinetics of the CD8 cytotoxic T cell response was similar when analyzed by ICS, ELISpot and tetramer binding. There was a minimal response up to 5 - 6 DPI, followed by a marked increase in cytokine-producing T cells particularly in the BAL (peak of 7.9% IFN $\gamma$  and 7.6% TNF at 9 DPI) and lung (peak of 1.3% IFN $\gamma$  and 0.6% TNF at 9 DPI). CD8 T-cells produced minimal IL-2 in all tissues except for BAL, where 0.7% to 1.3% positive cells were detected between 7 and 13 DPI. PBMC had much lower proportion of cytokine producing CD8 T cells with maximum 0.3% IFN $\gamma$  and 0.2% TNF production in PBMC at 9 DPI. The high cytokine responses

were maintained in BAL and lung until 21 DPI, with lower responses in the TBLN and none in PBMC (**Figure 3**).

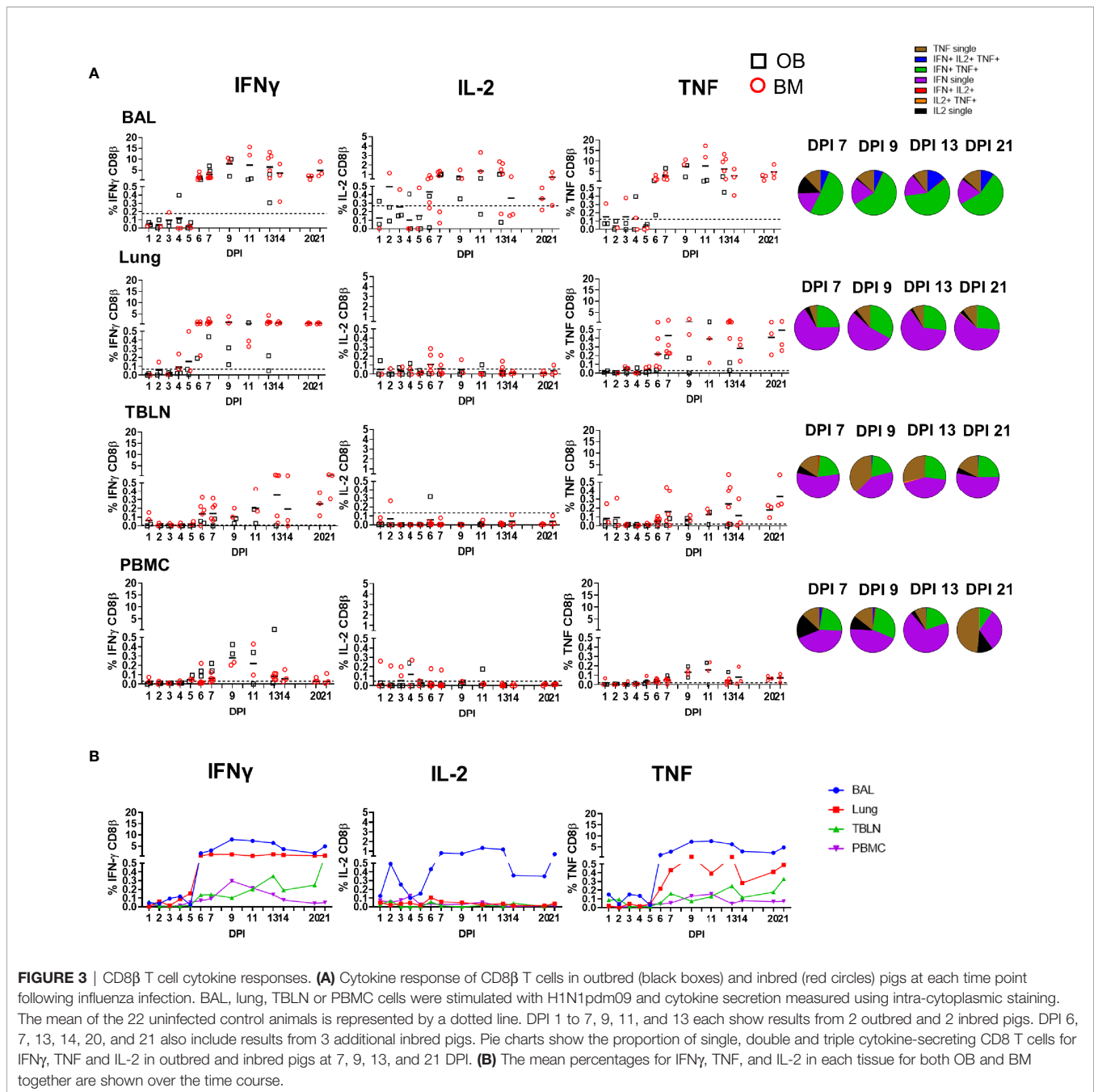
We next determined the quality of cytokine responses of CD8 $\beta$  T cells. The CD8 $\beta$  T-cell cytokine response was dominated by IFN $\gamma$  single producing cells with some IFN $\gamma$ /TNF double producing cells also present in all tissues (**Figure 3A**). However, the highest proportion of double IFN $\gamma$ /TNF producing cells was present in the BAL (**Table 2**). A triple secreting IFN $\gamma$ /IL-2/TNF population was detected only in the BAL and these cells produced greater levels of IFN $\gamma$  per cell as measured by MFI (**Supplementary Figure 2B**). The individual cytokine profiles of the BM and OB were similar during the time course of H1N1pdm09 infection and shown in **Supplementary Figure 3**. We also analyzed the responses in the in-contact animals from experiments OB1, OB2, BM1, and BM2. These animals had the same profiles of cytokine production in BAL (**Supplementary Figure 4**) and in the other tissues (data not shown) as directly challenged animals (**Table 3**).

The CD4 response was lower than the CD8 and developed earlier at 4 to 5 DPI in some animals (**Figure 4**). It was greatest in the BAL and peaked at 9 DPI similarly to CD8 (1.6% IFN $\gamma$  and 2.1% TNF) and almost disappeared by 21 DPI. The CD4 response was lower in TBLN, lung and PBMC (**Table 2**). CD4 cytokine secretion differed between tissues. Single cytokine-secreting IFN $\gamma$  and TNF CD4 T cells were dominant in the lung and TBLN respectively, while in the BAL and PBMC both single IFN $\gamma$ , single TNF and double IFN $\gamma$ /TNF were present. The individual cytokine profiles of the BM and OB animals were comparable (**Supplementary Figure 3**). The in-contacts also showed a similar pattern of cytokine production except for TNF (**Supplementary Figure 4, Table 3**).

These results demonstrate that there is a strong antigen specific CD8 T cell response in the local lung tissues and in particularly in the BAL. Cytokine production by CD8 was dominated by IFN $\gamma$  and TNF, but the BAL also had a significant population of IL-2-producing cells and more double- and triple-producing cells, compared to TBLN, lung and PBMC. The CD4 T cell response was also greatest in the BAL, although much lower and declining

**TABLE 1** | Antibodies used.

Antigen	Clone	Isotype	Fluorochrome	Source of primary Ab	Details of secondary Ab
<b>Staining for conventional T cells</b>					
<b>CD4</b>	74-12-4	IgG2b	PerCP-Cy5.5	BD Biosciences	
<b>CD8<math>\beta</math></b>	PPT23	IgG1	FITC	Bio-Rad Laboratories	
<b>TNF</b>	MAb11	IgG1	BV421	BioLegend	
<b>IFN<math>\gamma</math></b>	P2G10	IgG1	APC	BD Biosciences	
<b>IL-2</b>	A150D 3F1 2H2	IgG2a	PE-Cy7	ThermoFisher	rat-anti-mouse, IgG2a, BioLegend
<b>Staining for <math>\gamma\delta</math> T cells</b>					
<b>TCR <math>\gamma\delta</math></b>	PGBL22A	IgG1	PE-Cy7	Cambridge bioscience	rat-anti-mouse, IgG1, BioLegend
<b>CD8<math>\alpha</math></b>	76-2-11	IgG2a	FITC	BD Biosciences	
<b>CD2</b>	MSA4	IgG2a	PerCP-Cy5.5	Cambridge bioscience	rat-anti-mouse, IgG2a, BioLegend
<b>TNF</b>	MAb11	IgG1	BV421	BioLegend	
<b>IFN<math>\gamma</math></b>	P2G10	IgG1	APC	BD Biosciences	
<b>IL-17A</b>	SCPL1362	IgG1	PE	BD Biosciences	



more rapidly than the CD8 response. The cytokine responses were similar between the in-contact and directly infected animals, indicating the similarities between experimental intra-nasal challenge and natural infection. No differences in magnitude, kinetic and quality of cytokine responses were observed between the OB and BM animals.

### $\gamma\delta$ T-Cell Responses During H1N1pdm09 Infection in Pigs

The importance of  $\gamma\delta$  T cells in control of influenza infection has been demonstrated in mice and humans (37–40). In pigs  $\gamma\delta$  T cells

are a prominent population in blood and secondary lymphoid organs and can produce IFN $\gamma$ , TNF and IL-17A following polyclonal stimulation (41–43). Porcine  $\gamma\delta$  T cells have been divided into different subsets based on the expression of CD2 and CD8 $\alpha$  (44).

We measured IFN $\gamma$ , TNF and IL-17A production in CD2 $^+$   $\gamma\delta$  T cells immediately *ex vivo* and following H1N1pdm09 re-stimulation. The cytokine production by CD2 $^+$   $\gamma\delta$  T cells was very low (data not shown) and thus we focused on CD2 $^+$   $\gamma\delta$  T cells. *Ex vivo*, BAL CD2 $^+$   $\gamma\delta$  T cells, without H1N1pdm09 stimulation, secreted IFN $\gamma$  and TNF early post infection with the highest



**TABLE 2** | Comparison of different populations of T cells from Babraham pigs infected with H1N1pdm09 virus.

% T cells binding to tetramer or/ cytokineproducing		Days Post Infection (DPI)		
		6 DPI	7 DPI	13 DPI
CD8 $\beta$	NP <sub>290-298</sub>	no significant (P>0.05) differences*	BAL†>PBMC (P=0.01) lung>PBMC (P=0.04) lung>TBLN (P=0.04)	BAL>lung (P=0.04) BAL>TBLN (P=0.01) BAL>PMBC (P=0.01) lung>PMBC (P=0.01) TBLN>PMBC (P=0.01)
	IFN $\gamma$	BAL>PBMC (P=0.01) BAL>TBLN (P=0.01) lung>PBMC (P=0.01) lung>TBLN (P=0.03)	BAL>PBMC (P=0.01) BAL>TBLN (P=0.01) lung>PBMC (P=0.01) lung>TBLN (P=0.03)	BAL>PBMC (P=0.01) BAL>TBLN (P=0.01) lung>PBMC (P=0.01) lung>TBLN (P=0.03)
CD8 $\beta$	IL-2	no significant (P>0.05) differences	BAL> lung (P=0.06) BAL>PBMC (P=0.02) BAL>BM TBLN (P=0.02)	BAL>lung (P=0.01) BAL>PBMC (P=0.01) BAL>TBLN (P=0.01)
	TNF	BAL>lung (P=0.01) BAL>PBMC (P=0.01) BAL>TBLN (P=0.01) lung>PBMC (P=0.02)	BAL>lung (P=0.02) BAL>PBMC (P=0.01) BAL>TBLN (P=0.01) lung>PBMC (P=0.02)	BAL>lung (P=0.01) BAL>PBMC (P=0.01) BAL>TBLN (P=0.01) lung>PBMC (P=0.02)
	IFN $\gamma$	no significant (P>0.05) differences	lung>TBLN (P=0.02) lung>PBMC (P=0.01)	BAL>PBMC (P=0.06) lung>PBMC (P=0.06)
CD4	IL-2	BAL>PBMC (P=0.01) lung>PBMC (P=0.03) TBLN>PBMC (P=0.01)	BAL>PBMC (P=0.01) lung>PBMC (P=0.01) TBLN>PBMC (P=0.01)	BAL>PBMC (P=0.01) lung>PBMC (P=0.01) TBLN>PBMC (P=0.01)
	TNF	no significant (P>0.05) differences	no significant (P>0.05) differences	BAL>PBMC (P=0.06) TBLN> lung (P=0.06) TBLN>PBMC (P=0.02)
	IFN $\gamma$	no significant (P>0.05) differences	lung>TBLN (P=0.02) lung>PBMC (P=0.01)	BAL>PBMC (P=0.06) lung>PBMC (P=0.06)

\*P-values based on pairwise Wilcoxon rank-sum tests following a significant (P<0.05) Kruskal-Wallis test.

†BAL, broncho-alveolar lavage; PBMC, peripheral blood mononuclear cell; TBLN, tracheobronchial lymph node.

**TABLE 3** | Comparison of T cells in broncho-alveolar lavage from experimentally inoculated (I) and in-contact (C) Babraham (BM) and outbred (OB) pigs infected with H1N1pdm09 swine influenza virus.

T cells	% cells producing		
	IFN $\gamma$	TNF	IL-2 or IL-17a*
CD8 $\beta$	no significant (P>0.05) differences <sup>†</sup>	no significant (P>0.05) differences <sup>†</sup>	no significant (P>0.05) differences <sup>†</sup>
CD4	no significant (P>0.05) differences <sup>†</sup>	OB, C>BM, C (P=0.03) OB, C>BM, I (P=0.02)	no significant (P>0.05) differences <sup>†</sup>
$\gamma\delta$ <i>ex vivo</i>	no significant (P>0.05) differences <sup>†</sup>	no significant (P>0.05) differences <sup>†</sup>	not tested
$\gamma\delta$ H1N1pdm09 stimulated	no significant (P>0.05) differences <sup>†</sup>	no significant (P>0.05) differences <sup>†</sup>	no significant (P>0.05) differences <sup>†</sup>

\*IL-2 for CD8 $\beta$  and CD4 T cells; IL-17a for  $\gamma\delta$  T cells.

†P-values based on pairwise Wilcoxon rank-sum tests following a significant (P<0.05) Kruskal-Wallis test.

frequency of 0.6% IFN $\gamma$  and 1.6% TNF at 3 DPI. The cells co-produced IFN $\gamma$ /TNF at low levels (**Figure 5**). A minimal amount of IL-17A was detected in BAL and no IFN $\gamma$ , TNF or IL-17 in the other tissues *ex vivo* (data not shown).

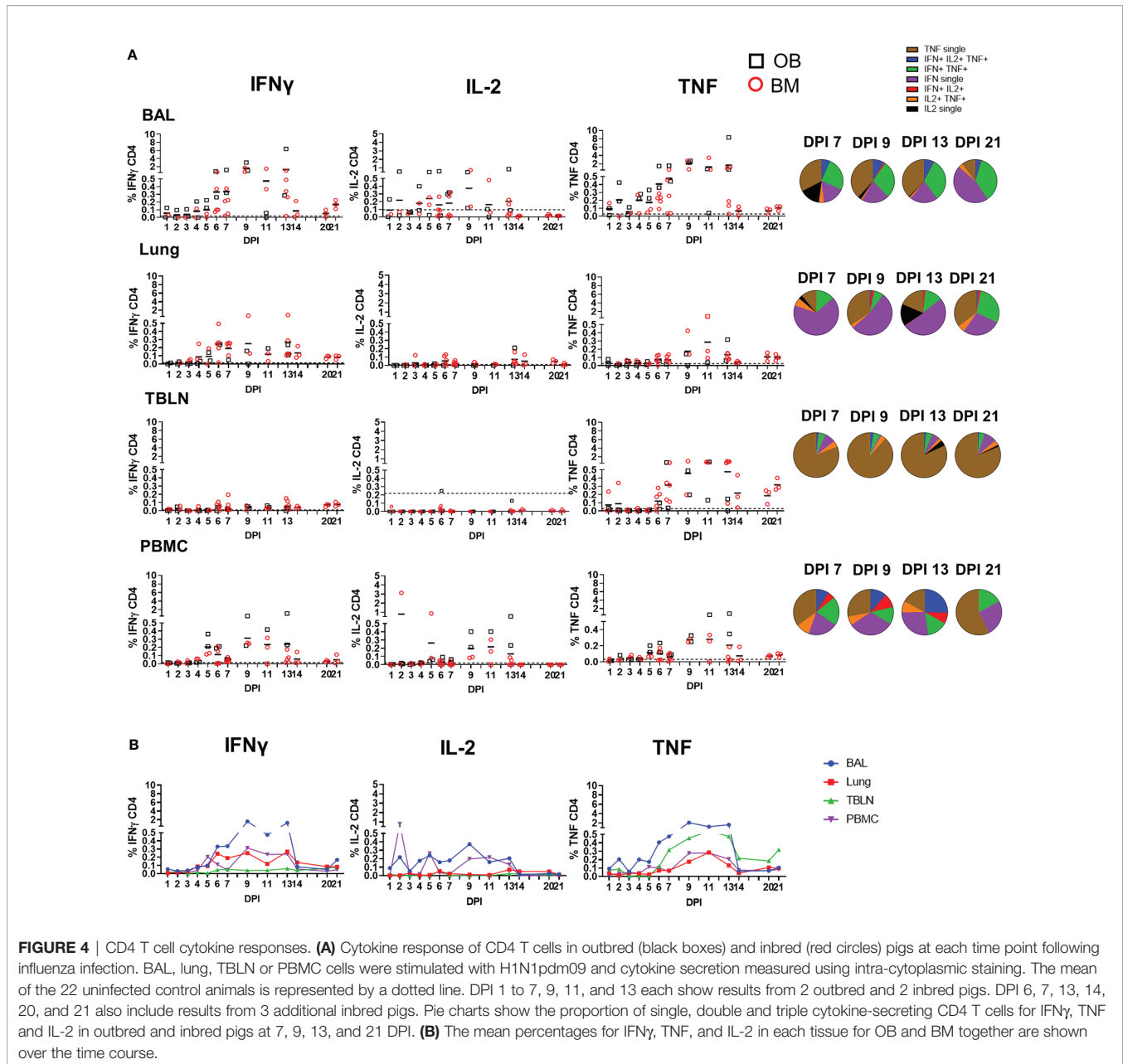
We also measured cytokine production after H1N1pdm09 stimulation *in vitro* and the highest proportion of IFN $\gamma$  producing cells was detected in BAL and lung at 7 DPI and maintained until 13 DPI (0.4% at 11 DPI for BAL) while in lung the highest frequency was 0.4% at 7 DPI (**Figure 6**). TNF showed similar pattern in BAL: increased at 9 DPI reaching a peak at 11 DPI with a mean of 0.7%. At later stages of infection, the frequency of cytokine producing cells were much lower. The majority of the H1N1pdm09 stimulated cells were IFN $\gamma$ /TNF co-producing (**Supplementary Figure 5**). The responses in the contacts (0.5% for IFN $\gamma$  and more than 1% for TNF) were similar to those in the directly challenged animals following H1N1pdm09 stimulation (**Table 3**). The proportion of IL-17A-

secreting CD2<sup>+</sup> cells was much lower compared to IFN $\gamma$  and TNF with the greatest response in the BAL at 11 DPI (0.2%).

Overall these data demonstrate that  $\gamma\delta$  T cells produce cytokines *ex vivo* early post infection, but that H1N1pdm09 *in vitro* stimulation increases cytokine production in CD2<sup>+</sup>  $\gamma\delta$  T cells from 7 to 13 DPI. No difference between OB and BM pigs were detected of response of *ex vivo* or stimulated  $\gamma\delta$  T cells.

## Antibody and B-Cell Responses During H1N1pdm09 Infection in Pigs

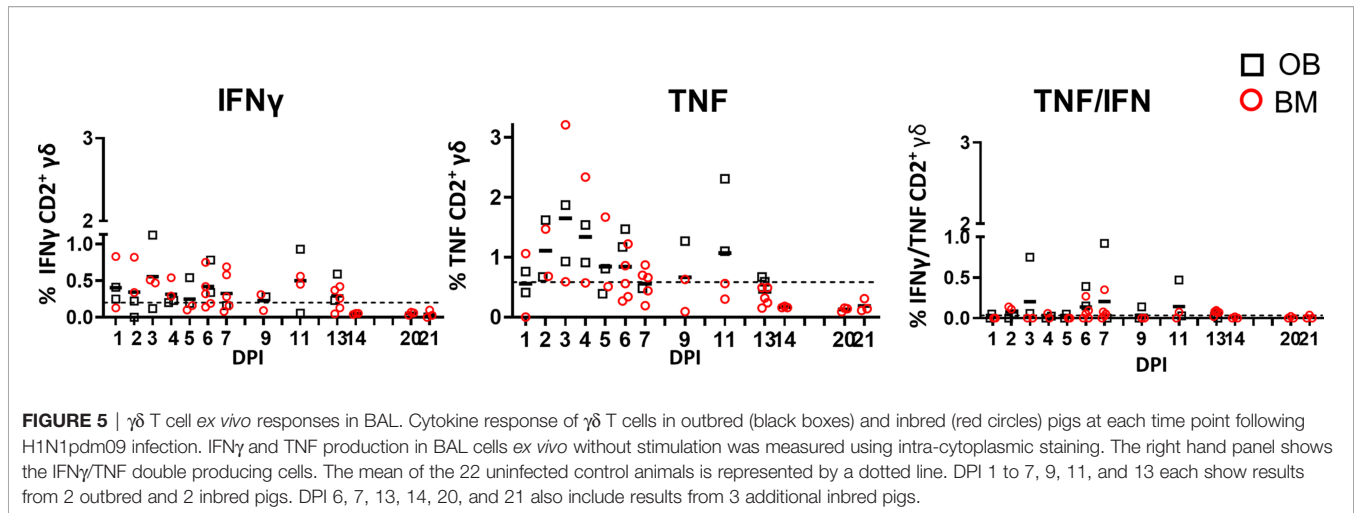
The antibody response after H1N1pdm09 infection was determined in serum, BAL and nasal swabs. Virus specific IgG and IgA were measured by end point titer ELISA against H1N1pdm09 virus or recombinant HA from H1N1pdm09/A/England/195/2009 (pH1) (**Figures 7A, B**). Serum IgG against H1N1pdm09 virus was detectable at 5 to 6 DPI, reached its peak at 14 DPI (1:13,650) and was maintained until 21 DPI (1:8,530).



IgA titers were lower compared to IgG. In contrast in BAL, IgG and IgA against H1N1pdm09 were present at the same levels. BAL IgG reached a peak of 1:2,370 at 13 DPI which was maintained up to 21 DPI. IgG and IgA were also measured in nasal swabs from experiment BM3 up to 9 DPI. Responses were detected at 6 DPI reaching a peak of 1:48 and 1:28 respectively by 9 DPI. We measured the ELISA response to pH1, which had a similar kinetic as the response to H1N1pdm09 virus but with approximately a log lower titer (**Figure 7B**). No significant differences in the upper asymptote, rate of increase in titer or time of maximum increase were detected for IgG or IgA between OB and BM, except for serum IgA H1N1 ELISA (upper asymptote OB 1:2,700 > BM 1:2,100,  $p=0.05$ ) (**Supplementary Table 1**).

To assess the breadth and cross-reactivity of the Ab, we tested the binding of sera from 21 DPI to MDCK cells expressing pH1, H5 (from A/Vietnam/1203/2004) and HA from PR8 in which, unlike in ELISA, the natural conformation of HA is maintained. There was strong binding to the MDCK expressing pH1 and weaker binding to H5 and HA from PR8 suggesting that H1N1pdm09 induces cross reactive responses to other group 1 H1 and H5 viruses (**Figure 7C**).

The function of antibodies in serum and BAL was tested by microneutralization (MN) assessing inhibition of virus entry, inhibition of hemagglutination (HAI) and inhibition of neuraminidase activity by enzyme-linked lectin assay (ELLA) (**Figure 8A**). MN was first detected in serum at 5 or 6 DPI mirroring Ab production in the tissues, increasing to 1:140 at 11



DPI at and 1:480 at 21 DPI. HAI and ELLA followed a similar pattern reaching 1:746 HAI or 1:160 ELLA at 21 DPI. BAL showed much lower MN, HAI and ELLA responses compared to serum. MN and ELLA titers in BAL peaked at 13 DPI and were maintained until 20 DPI. HAI reached a peak at 11 DPI and was undetectable at DPI 21. No significant differences in MN, HAI and ELLA in the upper asymptote, rate of increase in titer or time of maximum increase between OB and BM animals were detected (**Supplementary Table 1**).

To determine the major sites of Ab production following H1N1pdm09 infection BAL, lung, TBLN, spleen and PBMC from experiment BM3 were tested for total IgG and HA-specific Ab-secreting cells (ASC) (**Figure 8B**). IgG producing cells were detected in all tissues with a trend for increasing numbers over time up to 21 DPI. TBLN showed the highest frequency of HA specific ASC reaching 200 ASC/ $10^6$  cells at 20/21 DPI. Lung demonstrated a similar pattern but with 18 ASC/ $10^6$  cells at 20/21 DPI.

In summary a strong Ab response was detected in serum, which was dominated by IgG, while in BAL the ELISA titers of IgG and IgA were comparable. Antibodies cross reacted with HA from H1 and H5 viruses. Microneutralization, HAI and ELLA titers were much higher in serum than BAL. HA specific ASC were detected in TBLN and lung. No differences were observed in the Ab responses between OB and BM animals.

All raw data in numerical format is included as **Supplementary File 8** with tabs corresponding to each figure.

## DISCUSSION

In this study we investigated the kinetic and magnitude of T cell and Ab responses in respiratory tissues and blood in outbred Landrace x Hampshire cross and inbred Babraham pigs following H1N1pdm09 infection. The relationship between these parameters and the virus load is illustrated in **Figure 9**. After experimental infection with H1N1pdm09 virus shedding plateaued between 1 and 4 to 5 DPI, followed by a steep decline so that by 9 DPI no virus could be detected in any animal. An *ex*

*vivo*  $\gamma\delta$  T cell IFN $\gamma$  and TNF response was apparent from 2 DPI, although this declined by 7 DPI. In contrast, virus reactive IFN $\gamma$  producing  $\gamma\delta$  T cells were detected at 7 DPI and maintained to 13 DPI. Significant virus specific CD4 and CD8 T cell response were present at 6 DPI. Similarly, virus-specific IgG and IgA were detected in serum and BAL at 5 - 6 DPI by which time the viral load had declined by 2 to 3 logs. By the time of the peak of the T cell and Ab responses (9–14 DPI), no virus was detectable. These kinetics suggest that innate mechanisms, including perhaps early  $\gamma\delta$  T cell cytokine secretion, contain viral replication at a plateau level in the first 4 to 5 days post infection, while adaptive T and Ab responses contribute to the complete clearance of virus after 5 DPI in primary infection and prevent future infections by a more rapid secondary immune response.

Similar kinetics of adaptive T cell responses have been reported in mice, with antigen specific cells detected as early 4 to 5 days post infection, increasing in number between 5 and 12 DPI in lung tissues (45, 46). Experiments in mice have shown that depletion of B or CD8 T cells results in delayed clearance of IAV (47–50). CD4 T cells also contribute to control of influenza infection, although depletion of this cell subset alone only slightly delayed viral clearance (51–53). The strong CD8 and Ab responses detected in the present study suggest that these cell types are also important for viral clearance in pigs. This could be confirmed by depletions studies or cell transfer in inbred Babraham pigs.

Few studies have analyzed in depth the conventional T cell response in pigs. The most comprehensive study showed a low frequency of virus specific IFN $\gamma$  producing CD4 and CD8 in the lung as early as 4 DPI after H1N2 intratracheal challenge, reaching a peak at 9 DPI, with the highest response in lung compared to TBLN or PBMC (25). Here, for the first time, we have analyzed the cytokine responses in BAL as well as lung interstitial tissues, which showed a similar kinetic. However, the response in the BAL was much stronger in terms of frequency of cytokine producing T cells. The BAL T cells produced multiple cytokines and more per cell, indicating that they may be most efficient in clearing the virus. Cytokine production differed between CD8 and CD4 T cells and between BAL, lung, and TBLN, perhaps reflecting the extensive

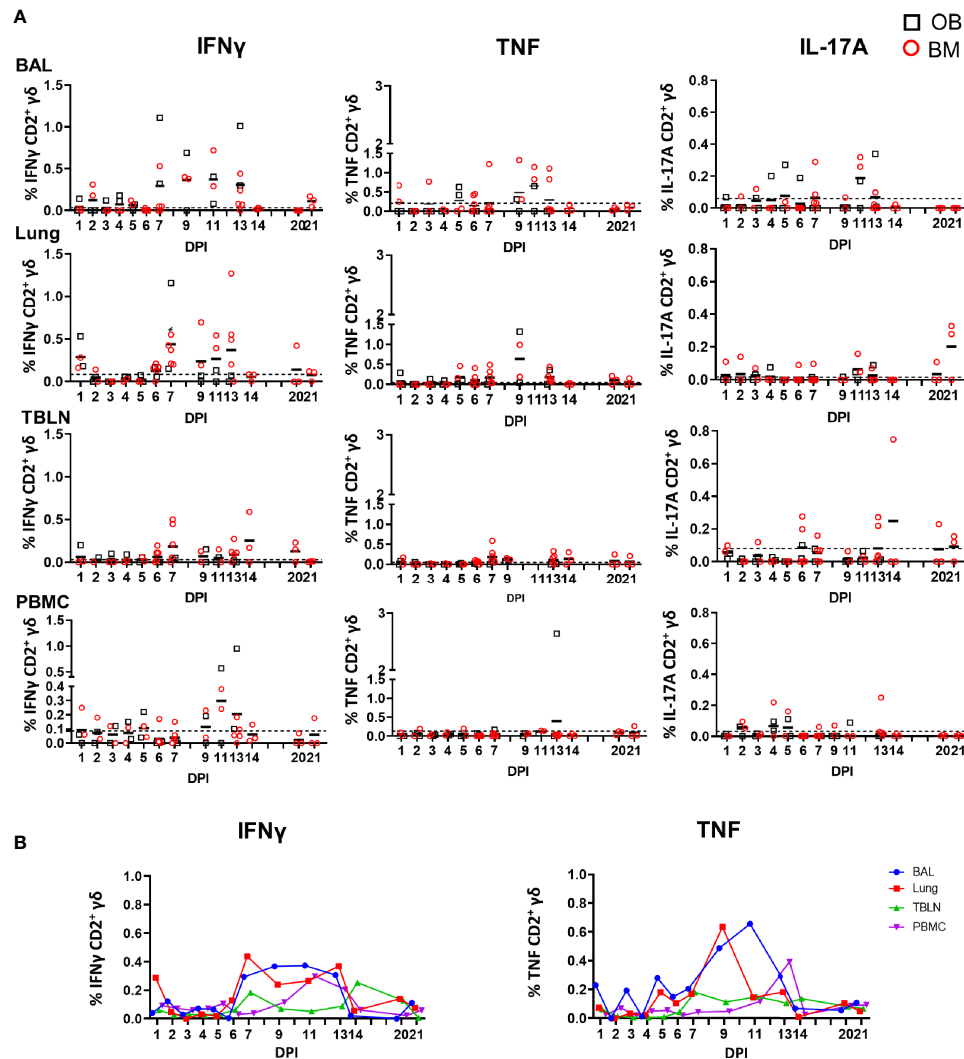


**FIGURE 6** |  $\gamma\delta$  T cell responses after H1N1pdm09 stimulation. **(A)** Frequencies of IFN $\gamma$ , TNF, and IL-17A-producing CD2 $^{+}$   $\gamma\delta$  T cells in outbred (black boxes) and inbred (red circles) pigs following influenza infection. BAL, lung, TBLN and PBMC were stimulated with H1N1pdm09 and cytokine secretion measured using intracytoplasmic staining. The mean of the 22 uninfected control animals is represented by a dotted line. DPI 1 to 7, 9, 11, and 13 each show results from 2 outbred and 2 inbred pigs. DPI 6, 7, 13, 14, 20, and 21 also include results from 3 additional inbred pigs. **(B)** Mean percentages for IFN $\gamma$  and TNF in each tissue are shown over the time course.

tissue compartmentalization in the respiratory tract and differential localization of CD4 and CD8 T cells (54). Whether specialized CD4 and CD8 T cells are compartmentalized due to the migration of different subsets to specific sites, as has been proposed in mice, or because tissue environments alter cytokine production remains to be established (55).

An important difference between the present study and Talker et al. is that they used the more pathogenic swine H1N2 virus, which was delivered in a large volume and high dose (15 ml of  $10^7$  TCID $_{50}$ /ml) intratracheally (25). This might explain the stronger and more prolonged lung, TBLN and PBMC responses they observed. The pigs in the present study were infected intranasally with a MAD and the response here was similar to the in-contact animals, suggesting that this method is

more similar to natural infection. Furthermore our scintigraphy study also indicates that this method of challenge targets both the upper and lower respiratory tract (56).

We detected a 27 times lower proportion of CD8 antigen-specific T cells in the blood compared to BAL. Similarly, antigen-specific CD8 T cells responses were much higher in the BAL of patients with H1N1pdm09 compared to blood (57). This indicates that sampling blood is not reflective of the true response in the lung and local tissues, which has implications for the design and analysis of clinical trials for T cell targeted vaccines. In contrast, CD4 responses were more similar in magnitude in blood and BAL, although less long lived than CD8.

In pigs,  $\gamma\delta$  T cells comprise up to 50% of lymphocytes in the blood (particularly in young animals) in contrast to humans

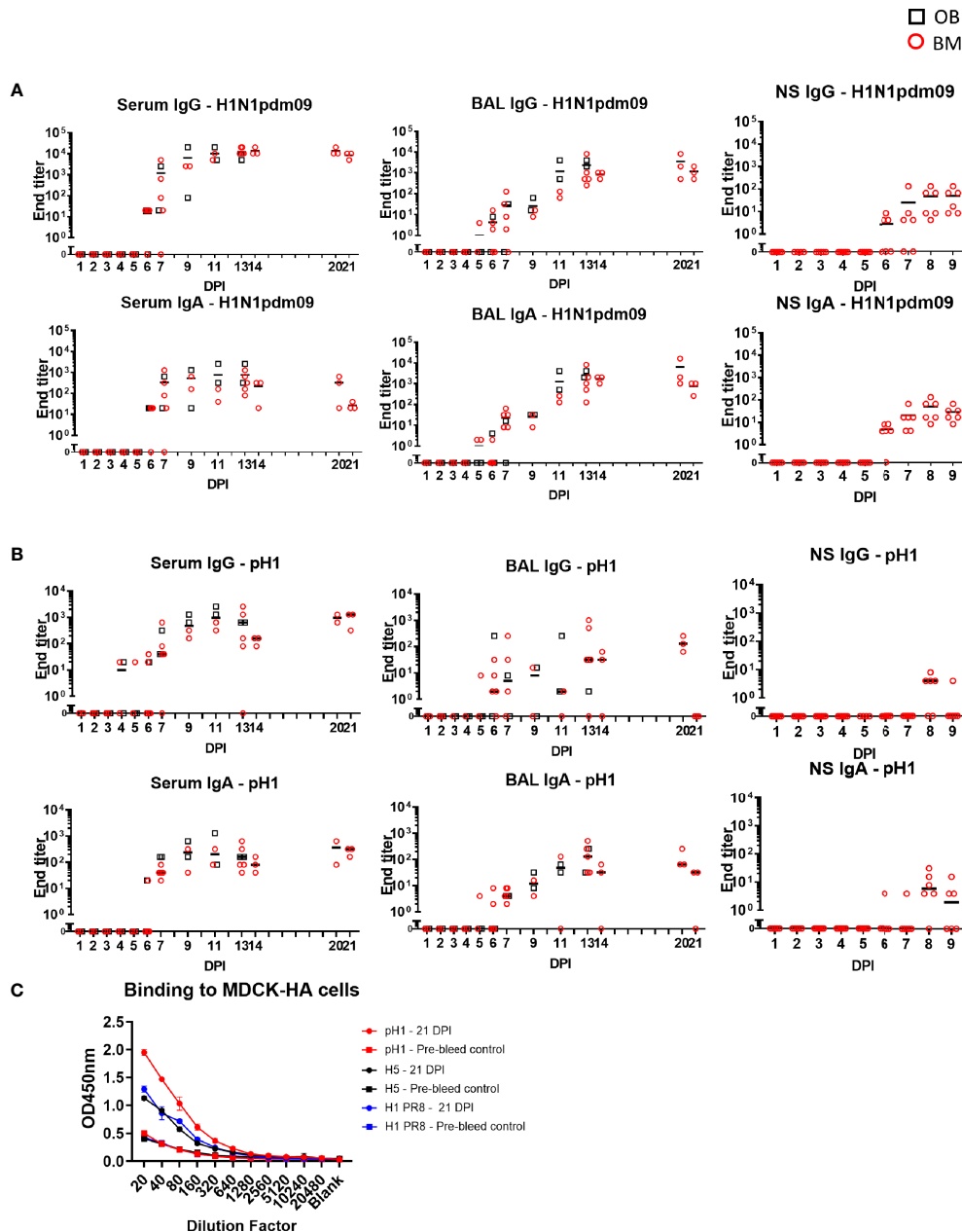
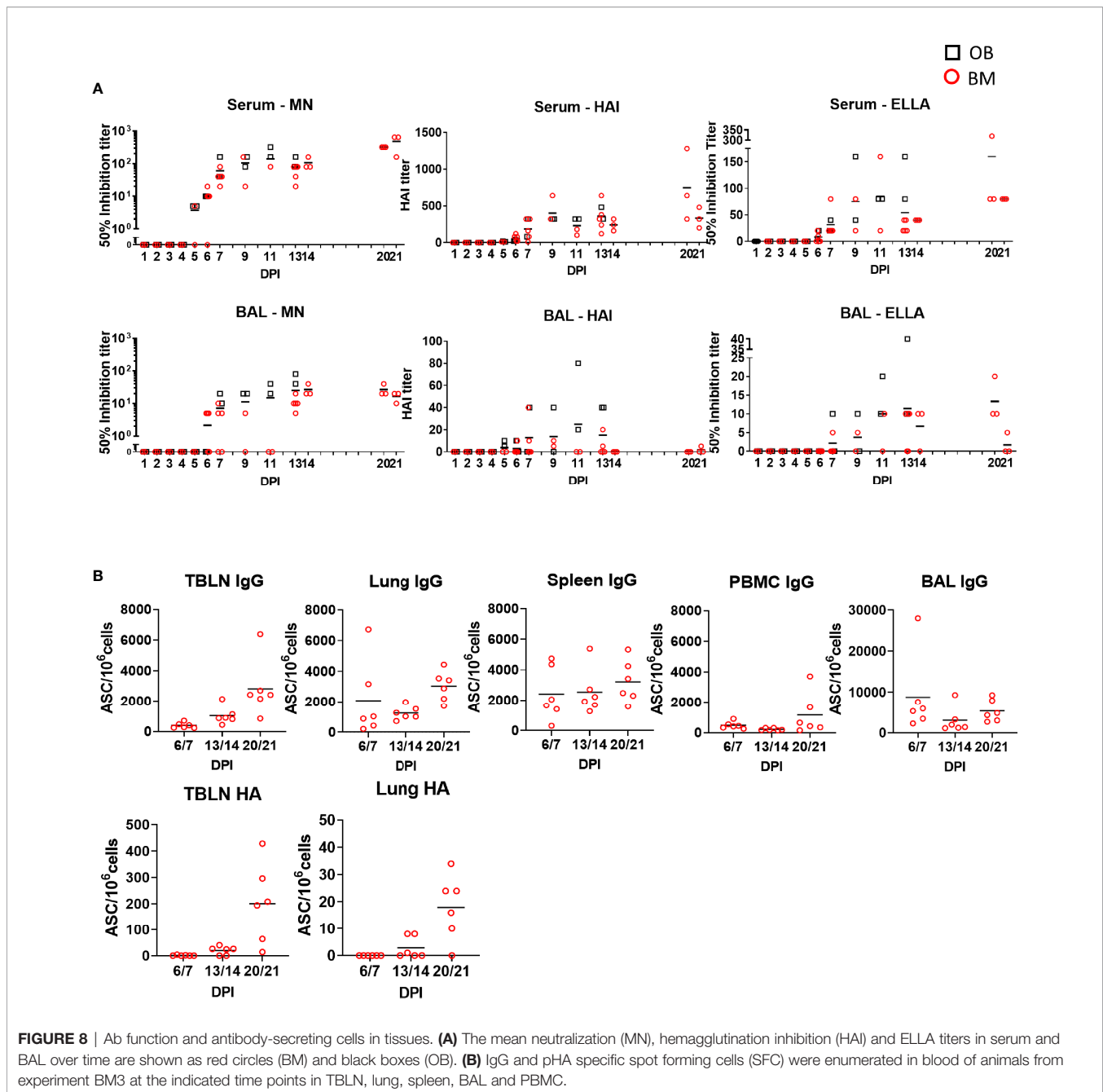


**FIGURE 7** | Ab ELISA responses and binding to MDCK-HA expressing cells. Influenza H1N1pdm09 virus specific IgA and IgG **(A)** and hemagglutinin (pH1) specific **(B)** responses in serum, BAL and nasal swabs (NS) were determined by ELISA and shown as black boxes (for OB) and red circles (for BM). NS were analyzed in BM3 only. **(C)** Binding of serum at 21 DPI to MDCK-pH1, MDCK-H1 PR8, and MDCK-H5 expressing cells.

where they usually represent 1% to 5% of lymphocytes (27, 58). The effect that this difference in the frequency of  $\gamma\delta$  T cells has in lung homeostasis and influenza immunity remains incompletely explored and must be considered when the pig is used as a model for human influenza.  $\gamma\delta$  T cell have previously been reported to increase late after IAV infection in mice, although an early increase in  $\gamma\delta$  T cells in mice and pigs has also been reported (26, 37, 38). Human  $\gamma\delta$  T cells can expand in a TCR-independent manner in response to IAV, and the human V $\gamma$ 9V $\delta$ 2 T cell subset

kills IAV-infected A549 airway cells (39). Although we did not observe a significant increase in  $\gamma\delta$  T cells after H1N1pdm09 infection, we showed that  $\gamma\delta$  T cells produce IFN $\gamma$  and TNF as early as day 2 post infection *ex vivo*, in agreement with studies in mice (40).  $\gamma\delta$  T cells are a major source for IL-17 production, which has been shown to play a role in IAV infection, but we detected only low levels of IL-17A after H1N1pdm09 stimulation of BAL cells (37, 59, 60). Surprisingly, we demonstrated that *in vitro* stimulation with H1N1pdm09 induces IFN $\gamma$  and TNF



production in  $CD2^+ \gamma\delta$  T cells from 7 to 13 DPI. This is reminiscent of an adaptive T cell response. Recombinant hemagglutinin from H5N1 has been previously demonstrated to activate human PBMC  $\gamma\delta$  T cells *in vitro* and this was not mediated by TCR or pattern recognition receptors (61). Further studies will elucidate the mechanisms of cytokine induction and whether it is TCR dependent.

H1N1pdm09 infection was characterized by high IgG and IgA titers in serum and BAL, and a detectable antibody titer in nasal swabs. The IgG titer was higher than IgA in serum, while similar levels of IgA and IgG were detected in BAL and nasal

swabs, suggesting local production of this isotype or more efficient translocation. Neutralization, HAI and neuraminidase inhibition titers peaked at 11 - 21 DPI. Our findings are in agreement with previous studies showing that in experimentally H1N1 infected pigs HA-specific antibodies peaked at 2 to 3 weeks (23). Similarly we detected HA-specific antibody-secreting cells in the local TBLN and lung tissues, but not PBMC (23). However, it might be that antibody-secreting cells are largely lost in these liquid nitrogen frozen and thawed samples.

Despite centuries of agricultural selective breeding, the pig has maintained a significant level of SLA genetic diversity, with

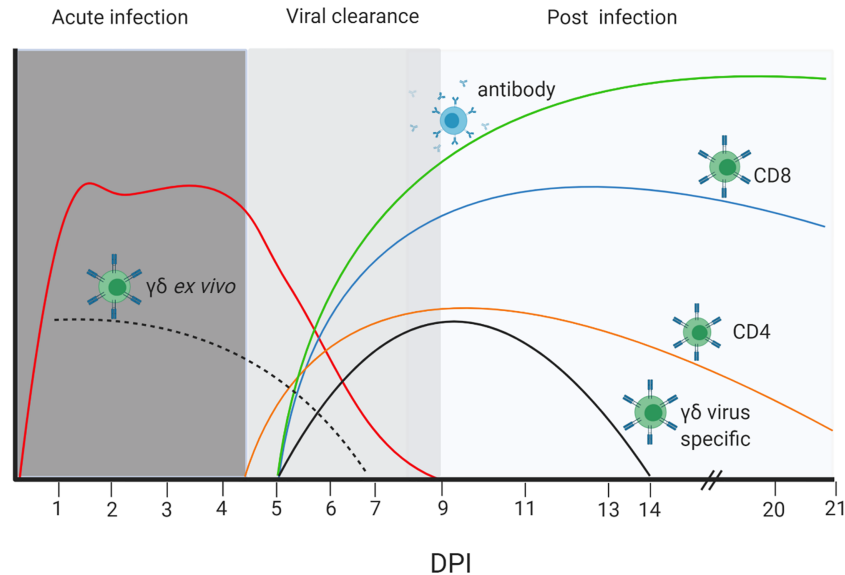


**FIGURE 9** | Dynamics of viral load, T cell and Ab responses. Stylized presentation of kinetics and magnitude of viral load and immune responses. The different color lines represent the antibody and cellular responses as indicated, and the red line the virus load. The dotted black line represents *ex vivo* cytokine production by  $\gamma\delta$  T cells, while the solid black line is the cytokine production by  $\gamma\delta$  T cells re-stimulated with H1N1pdm09 virus *in vitro*. The magnitude of responses and virus load are represented on an arbitrary scale. The figure was created with BioRender.com.

227 class I and 211 class II alleles identified for *Sus scrofa* in the Immuno-Polymorphism Database (IPD) MHC database to date, making analysis of the fine specificity of immune responses extremely difficult (62). The inbred Babraham line of pigs, on the other hand, is SLA homozygous for class I SLA-1\*14:02; SLA-2\*11:04 and SLA-3\*04:03 and class II DRB1-\*05:01, DQA-\*01:03, and DQB1-\*08:01 (19). This homozygosity enabled the use of peptide-SLA tetramers to the dominant NP antigen to track the CD8 response in tissues in this study (20). The  $\alpha\beta$ ,  $\gamma\delta$  T cell and Ab responses in the OB and BM animals were comparable, although there was lower proportion of CD8 T cells and higher proportion of  $\gamma\delta$  T cells in the BM pigs. This may be due to a genetic difference, although it may also be a result of different housing conditions, since the Babraham pigs are maintained under specific pathogen-free conditions, whereas the outbred pigs were obtained from a commercial breeder.

Our detailed analysis of immune responses in pigs showed that the viral load is contained in the period before the adaptive response is detectable, indicating the importance of innate immune mechanisms in influenza infection. As in other species however it appears that the adaptive response is essential for elimination of virus. BAL contains the most highly activated CD8, CD4, and  $\gamma\delta$  T cells producing large amounts of cytokines, which likely contribute to clearance of virus. We further show clear differences between the function of CD4, CD8, and  $\gamma\delta$  T cells between the lung, BAL and TBLN, while the blood is a poor representation of the local immune response. Although some differences were observed in the proportion of CD8 and  $\gamma\delta$  T cells in naïve outbred and Babraham pigs, we did not detect any differences in their immune response to H1N1pdm09 infection.

The availability of fine grain immunologic tools in Babraham pigs will allow the unraveling of immune mechanisms and confirm and extend findings in outbred populations.

## SLOLA INFLUENZA DYNAMICS CONSORTIUM

The sLoLa Influenza Dynamics consortium is (in alphabetical order): Mario Aramouni, Mick Bailey, Amy Boyd, Sharon Brookes, Ian Brown, Becky Clark, Bryan Charleston, Catherine Charreyre, Margo Chase-Topping, Federica Di-Palma, Matthew Edmans, Graham Etherington, Helen Everett, Ore Francis, Simon Frost, Sarah Gilbert, Ross Harley, Barbara Holzer, Adam McNee, Angela Man, Veronica Martini, Sophie Morgan, Emily Porter, Jin Qi Fu, Amy Thomas, Elma Tchilian, Laurence Tiley, Pauline van Diemen, James Wood, Fei Xiang.

## DATA AVAILABILITY STATEMENT

The raw data supporting the conclusions of this article will be made available by the authors, without undue reservation.

## ETHICS STATEMENT

The animal study was reviewed and approved by Pirbright Institute, and Bristol University. Written informed consent was obtained from the owners for the participation of their animals in this study.

## AUTHOR CONTRIBUTIONS

BC, MB, and ET conceived, designed and coordinated the study. BC, MB, ET, ME, AM, EP, EV, BP, VM OF, RH, AT, RB, and SM designed and performed experiments, processed samples, and analyzed the data. SG performed statistical analysis. AF and AS generated SLA tetramers. ET, ME, EV, and AM wrote and revised the manuscript and figures. All authors contributed to the article and approved the submitted version.

## FUNDING

This work was funded by the UKRI Biotechnology and Biological Sciences Research Council (BBSRC) grants: sLoLa BB/L001330/1, BBS/E/I/00007031, BBS/E/I/00007038, and BBS/E/I/00007039.

## REFERENCES

- Sun H, Xiao Y, Liu J, Wang D, Li F, Wang C, et al. Prevalent Eurasian avian-like H1N1 swine influenza virus with 2009 pandemic viral genes facilitating human infection. *Proc Natl Acad Sci U S A* (2020) 117(29):17204–10. doi: 10.1073/pnas.1921186117
- Kaplan BS, Kimble JB, Chang J, Anderson TK, Gauger PC, Janas-Martindale A, et al. Aerosol transmission from infected swine to ferrets of an H3N2 virus collected from an agricultural fair and associated with human variant infections. *J Virol* (2020) 94(16):JVI.01009–20. doi: 10.1128/jvi.01009-20
- Nelson MI, Vincent AL. Reverse zoonosis of influenza to swine: new perspectives on the human-animal interface. *Trends Microbiol* (2015) 23(3):142–53. doi: 10.1016/j.tim.2014.12.002
- Anderson TK, Chang J, Arendsee ZW, Venkatesh D, Souza CK, Kimble JB, et al. Swine Influenza A Viruses and the Tangled Relationship with Humans. *Cold Spring Harb Perspect Med* (2020) a038737. doi: 10.1101/cshperspect.a038737
- Smith GJ, Vijaykrishna D, Bahl J, Lycett SJ, Worobey M, Pybus OG, et al. Origins and evolutionary genomics of the 2009 swine-origin H1N1 influenza A epidemic. *Nature* (2009) 459(7250):1122–5. doi: 10.1038/nature08182
- Mifsud EJ, Tai CM, Hurt AC. Animal models used to assess influenza antivirals. *Expert Opin Drug Discovery* (2018) 13(12):1131–9. doi: 10.1080/17460441.2018.1540586
- Hemmink JD, Whittaker CJ, Shelton HA. Animal Models in Influenza Research. *Methods Mol Biol* (2018) 1836:401–30. doi: 10.1007/978-1-4939-8678-1\_20
- Bouvier NM, Lowen AC. Animal Models for Influenza Virus Pathogenesis and Transmission. *Viruses* (2010) 2(8):1530–63. doi: 10.3390/v20801530
- Margine I, Krammer F. Animal models for influenza viruses: implications for universal vaccine development. *Pathogens* (2014) 3(4):845–74. doi: 10.3390/pathogens3040845
- Lewis NS, Russell CA, Langat P, Anderson TK, Berger K, Bielejec F, et al. The global antigenic diversity of swine influenza A viruses. *Elife* (2016) 5:e12217. doi: 10.7554/eLife.12217
- Watson SJ, Langat P, Reid SM, Lam TT, Cotten M, Kelly M, et al. Molecular Epidemiology and Evolution of Influenza Viruses Circulating within European Swine between 2009 and 2013. *J Virol* (2015) 89(19):9920–31. doi: 10.1128/JVI.00840-15
- Janke BH. Influenza A virus infections in swine: pathogenesis and diagnosis. *Vet Pathol* (2014) 51(2):410–26. doi: 10.1177/0300985813513043
- Rajao DS, Vincent AL. Swine as a model for influenza A virus infection and immunity. *ILAR J* (2015) 56(1):44–52. doi: 10.1093/ilar/ilv002
- Canini L, Holzer B, Morgan S, Dinie Hemmink J, Clark B, Woolhouse MEJ, et al. Timelines of infection and transmission dynamics of H1N1pdm09 in swine. *PLoS Pathog* (2020) 16(7):e1008628. doi: 10.1371/journal.ppat.1008628
- McNee A, Smith TRF, Holzer B, Clark B, Bessell E, Guibinga G, et al. Establishment of a Pig Influenza Challenge Model for Evaluation of Monoclonal

## ACKNOWLEDGMENTS

We are grateful to animal staff at Langford School of Veterinary for providing excellent animal care. We are grateful to Alain Townsend for providing recombinant HAs and H7N1 virus. We thank APHA for providing the swine A/Sw/Eng/1353/09 influenza virus strain (DEFRA surveillance program SW3401).

## SUPPLEMENTARY MATERIAL

The Supplementary Material for this article can be found online at: <https://www.frontiersin.org/articles/10.3389/fimmu.2020.604913/full#supplementary-material>

- Antibody Delivery Platforms. *J Immunol* (2020) 205(3):648–60. doi: 10.4049/jimmunol.2000429
- Choi NR, Seo DW, Choi KM, Ko NY, Kim JH, Kim HI, et al. Analysis of Swine Leukocyte Antigen Haplotypes in Yucatan Miniature Pigs Used as Biomedical Model Animal. *Asian Australas J Anim Sci* (2016) 29(3):321–6. doi: 10.5713/ajas.15.0331
  - Sachs DH, Leight G, Cone J, Schwarz S, Stuart L, Rosenberg S. Transplantation in miniature swine. I. Fixation of the major histocompatibility complex. *Transplantation* (1976) 22(6):559–67. doi: 10.1097/00007890-197612000-00004
  - Signer EN, Jeffreys AJ, Licence S, Miller R, Byrd P, Binns R. DNA profiling reveals remarkably low genetic variability in a herd of SLA homozygous pigs. *Res Vet Sci* (1999) 67(2):207–11. doi: 10.1053/rvsc.1999.0310
  - Schwartz JC, Hemmink JD, Graham SP, Tchilian E, Charleston B, Hammer SE, et al. The major histocompatibility complex homozygous inbred Babraham pig as a resource for veterinary and translational medicine. *HLA* (2018) 92(1):40–3. doi: 10.1111/tan.13281
  - Tungatt K, Dolton G, Morgan SB, Attaf M, Fuller A, Whalley T, et al. Induction of influenza-specific local CD8 T-cells in the respiratory tract after aerosol delivery of vaccine antigen or virus in the Babraham inbred pig. *PLoS Pathog* (2018) 14(5):e1007017. doi: 10.1371/journal.ppat.1007017
  - Binns RM, Blakeley D, Licence ST. Migration of fluoresceinated pig lymphocytes in vivo: technical aspects and use in studies of autologous and homologous cell survival for up to three weeks. *Int Arch Allergy Appl Immunol* (1981) 66(3):341–9. doi: 10.1159/000232839
  - Heinen PP, van Nieuwstadt AP, Pol JM, de Boer-Luijtz EA, van Oirschot JT, Bianchi AT. Systemic and mucosal isotype-specific antibody responses in pigs to experimental influenza virus infection. *Viral Immunol* (2000) 13(2):237–47. doi: 10.1089/vim.2000.13.237
  - Larsen DL, Karasin A, Zuckermann F, Olsen CW. Systemic and mucosal immune responses to H1N1 influenza virus infection in pigs. *Vet Microbiol* (2000) 74(1-2):117–31. doi: 10.1016/S0378-1135(00)00172-3
  - Talker SC, Koinig HC, Stadler M, Graage R, Klingler E, Ladinig A, et al. Magnitude and kinetics of multifunctional CD4+ and CD8beta+ T cells in pigs infected with swine influenza A virus. *Vet Res* (2015) 46(1):52. doi: 10.1186/s13567-015-0182-3
  - Talker SC, Stadler M, Koinig HC, Mair KH, Rodriguez-Gomez IM, Graage R, et al. Influenza A Virus Infection in Pigs Attracts Multifunctional and Cross-Reactive T Cells to the Lung. *J Virol* (2016) 90(20):9364–82. doi: 10.1128/jvi.01211-16
  - Khatri M, Dwivedi V, Krakowka S, Manickam C, Ali A, Wang L, et al. Swine influenza H1N1 virus induces acute inflammatory immune responses in pig lungs: a potential animal model for human H1N1 influenza virus. *J Virol* (2010) 84(21):11210–8. doi: 10.1128/JVI.01211-10
  - Schwaiger T, Sehl J, Karte C, Schäfer A, Hühr J, Mettenleiter TC, et al. Experimental H1N1pdm09 infection in pigs mimics human seasonal influenza infections. *PLoS One* (2019) 14(9):e0222943. doi: 10.1371/journal.pone.0222943



28. Holzer B, Morgan SB, Matsuoka Y, Edmans M, Salguero FJ, Everett H, et al. Comparison of Heterosubtypic Protection in Ferrets and Pigs Induced by a Single-Cycle Influenza Vaccine. *J Immunol* (2018) 200(12):4068–77. doi: 10.4049/jimmunol.1800142
29. Morgan SB, Hemmink JD, Porter E, Harley R, Shelton H, Aramouni M, et al. Aerosol Delivery of a Candidate Universal Influenza Vaccine Reduces Viral Load in Pigs Challenged with Pandemic H1N1 Virus. *J Immunol* (2016) 196(12):5014–23. doi: 10.4049/jimmunol.1502632
30. Huang KY, Rijal P, Schimanski L, Powell TJ, Lin TY, McCauley JW, et al. Focused antibody response to influenza linked to antigenic drift. *J Clin Invest* (2015) 125(7):2631–45. doi: 10.1172/jci81104
31. Powell TJ, Silk JD, Sharps J, Fodor E, Townsend AR. Pseudotyped influenza A virus as a vaccine for the induction of heterotypic immunity. *J Virol* (2012) 86(24):13397–406. doi: 10.1128/jvi.01820-12
32. Bates D, Mächler M, Bolker B, Walker S. Fitting Linear Mixed-Effects Models Using lme4. *J Stat Software* (2015) 67(1):1–48. doi: 10.18637/jss.v067.i01
33. Hayward AC, Wang L, Goonetilleke N, Fragaszy EB, Bermingham A, Copas A, et al. Natural T Cell-mediated Protection against Seasonal and Pandemic Influenza. Results of the Flu Watch Cohort Study. *Am J Respir Crit Care Med* (2015) 191(12):1422–31. doi: 10.1164/rccm.201411-1988OC
34. Sridhar S, Begom S, Bermingham A, Hoschler K, Adamson W, Carman W, et al. Cellular immune correlates of protection against symptomatic pandemic influenza. *Nat Med* (2013) 19(10):1305–12. doi: 10.1038/nm.3350
35. McMichael AJ, Gotch FM, Noble GR, Beare PA. Cytotoxic T-cell immunity to influenza. *N Engl J Med* (1983) 309(1):13–7. doi: 10.1056/nejm198307073090103
36. Holzer B, Martini V, Edmans M, Tchilian E. T and B Cell Immune Responses to Influenza Viruses in Pigs. *Front Immunol* (2019) 10:98. doi: 10.3389/fimmu.2019.00098
37. Palomino-Segura M, Latino I, Farsakoglu Y, Gonzalez SF. Early production of IL-17A by  $\gamma\delta$  T cells in the trachea promotes viral clearance during influenza infection in mice. *Eur J Immunol* (2020) 50(1):97–109. doi: 10.1002/eji.201948157
38. Carding SR, Allan W, Kyes S, Hayday A, Bottomly K, Doherty PC. Late dominance of the inflammatory process in murine influenza by gamma/delta + T cells. *J Exp Med* (1990) 172(4):1225–31. doi: 10.1084/jem.172.4.1225
39. Li H, Xiang Z, Feng T, Li J, Liu Y, Fan Y, et al. Human Vgamma9Vdelta2-T cells efficiently kill influenza virus-infected lung alveolar epithelial cells. *Cell Mol Immunol* (2013) 10(2):159–64. doi: 10.1038/cmi.2012.70
40. Xue C, Wen M, Bao L, Li H, Li F, Liu M, et al. V $\gamma$ 4(+)  $\gamma\delta$ T Cells Aggravate Severe H1N1 Influenza Virus Infection-Induced Acute Pulmonary Immunopathological Injury via Secreting Interleukin-17A. *Front Immunol* (2017) 8:1054. doi: 10.3389/fimmu.2017.01054
41. Gerner W, Käser T, Saalmüller A. Porcine T lymphocytes and NK cells—an update. *Dev Comp Immunol* (2009) 33(3):310–20. doi: 10.1016/j.dci.2008.06.003
42. Sedlak C, Patzl M, Saalmüller A, Gerner W. CD2 and CD8 $\alpha$  define porcine  $\gamma\delta$  T cells with distinct cytokine production profiles. *Dev Comp Immunol* (2014) 45(1):97–106. doi: 10.1016/j.dci.2014.02.008
43. Takamatsu HH, Denyer MS, Stirling C, Cox S, Aggarwal N, Dash P, et al. Porcine gammadelta T cells: possible roles on the innate and adaptive immune responses following virus infection. *Vet Immunol Immunopathol* (2006) 112(1–2):49–61. doi: 10.1016/j.vetimm.2006.03.011
44. Stepanova K, Sinkora M. Porcine  $\gamma\delta$  T lymphocytes can be categorized into two functionally and developmentally distinct subsets according to expression of CD2 and level of TCR. *J Immunol* (2013) 190(5):2111–20. doi: 10.4049/jimmunol.1202890
45. Miao H, Hollenbaugh JA, Zand MS, Holden-Wiltse J, Mosmann TR, Perelson AS, et al. Quantifying the early immune response and adaptive immune response kinetics in mice infected with influenza A virus. *J Virol* (2010) 84(13):6687–98. doi: 10.1128/jvi.00266-10
46. Lawrence CW, Ream RM, Braciale TJ. Frequency, specificity, and sites of expansion of CD8+ T cells during primary pulmonary influenza virus infection. *J Immunol* (2005) 174(9):5332–40. doi: 10.4049/jimmunol.174.9.5332
47. Eichelberger M, Allan W, Zijlstra M, Jaenisch R, Doherty PC. Clearance of influenza virus respiratory infection in mice lacking class I major histocompatibility complex-restricted CD8+ T cells. *J Exp Med* (1991) 174(4):875–80. doi: 10.1084/jem.174.4.875
48. Sarawar SR, Sangster M, Coffman RL, Doherty PC. Administration of anti-IFN-gamma antibody to beta 2-microglobulin-deficient mice delays influenza virus clearance but does not switch the response to a T helper cell 2 phenotype. *J Immunol* (1994) 153(3):1246–53.
49. Bender BS, Croghan T, Zhang L, Small PA Jr. Transgenic mice lacking class I major histocompatibility complex-restricted T cells have delayed viral clearance and increased mortality after influenza virus challenge. *J Exp Med* (1992) 175(4):1143–5. doi: 10.1084/jem.175.4.1143
50. Graham MB, Braciale TJ. Resistance to and recovery from lethal influenza virus infection in B lymphocyte-deficient mice. *J Exp Med* (1997) 186(12):2063–8. doi: 10.1084/jem.186.12.2063
51. Topham DJ, Tripp RA, Sarawar SR, Sangster MY, Doherty PC. Immune CD4+ T cells promote the clearance of influenza virus from major histocompatibility complex class II -/- respiratory epithelium. *J Virol* (1996) 70(2):1288–91. doi: 10.1128/jvi.70.2.1288-1291.1996
52. Román E, Miller E, Harmsen A, Wiley J, Von Andrian UH, Huston G, et al. CD4 effector T cell subsets in the response to influenza: heterogeneity, migration, and function. *J Exp Med* (2002) 196(7):957–68. doi: 10.1084/jem.20021052
53. Jelley-Gibbs DM, Dibble JP, Filipson S, Haynes L, Kemp RA, Swain SL. Repeated stimulation of CD4 effector T cells can limit their protective function. *J Exp Med* (2005) 201(7):1101–12. doi: 10.1084/jem.20041852
54. Topham DJ, Reilly EC. Tissue-Resident Memory CD8+ T Cells: From Phenotype to Function. *Front Immunol* (2018) 9:515. doi: 10.3389/fimmu.2018.00515
55. Strutt TM, McKinstry KK, Marshall NB, Vong AM, Dutton RW, Swain SL. Multipronged CD4(+) T-cell effector and memory responses cooperate to provide potent immunity against respiratory virus. *Immunol Rev* (2013) 255(1):149–64. doi: 10.1111/imr.12088
56. Martini V, Hinchcliffe M, Blackshaw E, Joyce M, McNea A, Beverley P, et al. Distribution of Droplets and Immune Responses After Aerosol and Intra-Nasal Delivery of Influenza Virus to the Respiratory Tract of Pigs. *Front Immunol* (2020) 11(2798):594470. doi: 10.3389/fimmu.2020.594470
57. Zhao Y, Zhang YH, Denney L, Young D, Powell TJ, Peng YC, et al. High levels of virus-specific CD4+ T cells predict severe pandemic influenza A virus infection. *Am J Respir Crit Care Med* (2012) 186(12):1292–7. doi: 10.1164/rccm.201207-1245OC
58. Roden AC, Morice WG, Hanson CA. Immunophenotypic attributes of benign peripheral blood gammadelta T cells and conditions associated with their increase. *Arch Pathol Lab Med* (2008) 132(11):1774–80. doi: 10.1043/1543-2165-132.11.1774
59. Li C, Yang P, Sun Y, Li T, Wang C, Wang Z, et al. IL-17 response mediates acute lung injury induced by the 2009 pandemic influenza A (H1N1) virus. *Cell Res* (2012) 22(3):528–38. doi: 10.1038/cr.2011.165
60. Crowe CR, Chen K, Pociask DA, Alcorn JF, Krivich C, Enelow RI, et al. Critical role of IL-17RA in immunopathology of influenza infection. *J Immunol* (2009) 183(8):5301–10. doi: 10.4049/jimmunol.0900995
61. Lu Y, Li Z, Ma C, Wang H, Zheng J, Cui L, et al. The interaction of influenza H5N1 viral hemagglutinin with sialic acid receptors leads to the activation of human  $\gamma\delta$  T cells. *Cell Mol Immunol* (2013) 10(6):463–70. doi: 10.1038/cmi.2013.26
62. Maccari G, Robinson J, Ballingall K, Guethlein LA, Grimholt U, Kaufman J, et al. IPD-MHC 2.0: an improved inter-species database for the study of the major histocompatibility complex. *Nucleic Acids Res* (2017) 45(D1):D860–d4. doi: 10.1093/nar/gkw1050

**Conflict of Interest:** The authors declare that the research was conducted in the absence of any commercial or financial relationships that could be construed as a potential conflict of interest.

Copyright © 2021 Edmans, McNea, Porter, Vatzia, Paudyal, Martini, Gubbins, Francis, Harley, Thomas, Burt, Morgan, Fuller, Sewell, Charlestone, Bailey and Tchilian. This is an open-access article distributed under the terms of the Creative Commons Attribution License (CC BY). The use, distribution or reproduction in other forums is permitted, provided the original author(s) and the copyright owner(s) are credited and that the original publication in this journal is cited, in accordance with accepted academic practice. No use, distribution or reproduction is permitted which does not comply with these terms.